

DMD # 81539

Complete substrate inhibition of cytochrome P450 2C8 by AZD9496, an oral selective estrogen receptor degrader

Tashinga E. Bapiro, Andy Sykes, Scott Martin, Michael Davies, James W. T. Yates, Matthias Hoch, Helen E. Rollison and Barry Jones

Oncology, IMED Biotech Unit, AstraZeneca, Cambridge, UK (T.E.B, A.S, S.M, M.D, J.W.T.Y, B.J)

Quantitative Clinical Pharmacology, Early Clinical Development, IMED Biotech Unit, AstraZeneca, Cambridge, UK (M.H)

Drug Safety and Metabolism, IMED Biotech Unit, AstraZeneca, Cambridge, UK (H.E.R)

DMD # 81539

Running title: Complete substrate inhibition of CYP2C8 by AZD9496

Corresponding Author:

Dr. Tashinga E. Bapiro

Oncology IMED Biotech Unit, AstraZeneca

Hodgkin Building c/o B310, Cambridge Science Park, Milton Road, Cambridge

CB4 0WG, UK

Email: tashinga.bapiro1@astrazeneca.com

Phone: +44 1625237218

Word count

Number of text pages: 31

Number of tables: 2

Number of figures: 8

Number of references: 33

Number of words in abstract: 241

Number of words in introduction: 744

Number of words in discussion: 1325

Abbreviations: AQN, amodiaquine; AUC, Area under the concentration time curve; CL_{int} , Intrinsic clearance; CYP, Cytochrome P450; ER, estrogen receptor; HLM, Human liver microsomes; K_i , Inhibitor constant; K_m , Michaelis constant; M-M, Michaelis-Menten; rCYP, recombinant cytochrome P450; SERD selective estrogen receptor degrader

Abstract

AZD9496 is an oral selective estrogen receptor degrader currently in clinical development for treatment of estrogen receptor positive breast cancer. In a first-in-human Phase 1 study, AZD9496 exhibited dose non-linear pharmacokinetics whose mechanistic basis was investigated in this study. The metabolism kinetics of AZD9496 were studied using human liver microsomes (HLM), recombinant cytochrome P450s (rCYPs) and hepatocytes. In addition, modelling approaches were used to gain further mechanistic insights. CYP2C8 was predominantly responsible for biotransformation of AZD9496 to its two main metabolites whose rate of formation with increasing AZD9496 concentrations exhibited complete substrate inhibition in HLM, rCYP2C8 and hepatocytes. Total inhibition by AZD9496 of amodiaquine *N*-deethylation, a specific probe of CYP2C8 activity confirmed the completeness of this inhibition. The commonly used substrate inhibition model analogous to uncompetitive inhibition, fitted poorly to the data. However, using the same model but without constraints on the number of molecules occupying the inhibitory binding site (i.e. nS_{1ES}) provided a significantly better fit (F test, $P < 0.005$). With the improved model, up to three AZD9496 molecules were predicted to bind the inhibitory site of CYP2C8. In contrast to previous studies showing substrate inhibition of CYPs to be partial, our results demonstrate complete substrate inhibition of CYP2C8 via binding of more than one molecule of AZD9496 to the inhibitory site. As CYP2C8 appears to be the sole isoform catalysing formation of the main metabolites, the substrate inhibition might explain the observed dose non-linearity in the clinic at higher doses.

Introduction

The cytochrome P450 (CYP) superfamily of enzymes is one of the best characterised enzyme systems with a diverse list of substrates that includes over 75% of currently used drugs whose pharmacokinetics they may thus impact (Rendic and Guengerich, 2015). The utility of the drug-CYP interaction knowledge such as avoidance of drug combinations likely to cause adverse effects due to altered pharmacokinetics is now well documented (Pelkonen et al., 2005). Indeed potential drug-CYP interaction studies are an important part of modern drug development programs and one of the aims of such studies is to provide an understanding of the kinetics of metabolism which in turn can be used to predict the clearance (Obach et al., 1997; Obach and Reed-Hagen, 2002).

The rates of most CYP-catalysed reactions can be described by the Michaelis-Menten (M-M) model in which the rate of product formation increases with increasing substrate concentration to a maximum (Venkatakrishnan et al., 2001). The key kinetic parameters K_m and V_{max} can be determined *in vitro* (Houston, 1994), however, the data needs to be carefully examined to ascertain whether fitting to the M-M equation provides the best estimates of the parameters. For some CYP-catalysed reactions, the apparent maximum rate of product formation is not maintained with further increase in substrate but decreases due to enzyme inhibition by the substrate itself (Spracklin et al., 1997; Tang et al., 2000).

Substrate inhibition of CYPs is generally considered partial and not complete as product formation, although reduced, remains measurable with increasing substrate concentration (Tang et al., 2000; Lin et al., 2001). The basis for substrate inhibition of CYPs is generally thought to involve binding to a productive and inhibitory site (Korzekwa et al., 1998) with binding to the inhibitory site thought to cause a conformational change that affects binding to

the productive site (Williams et al., 2004). For CYPs that have large active sites, it is not inconceivable for both sites to be located in close proximity within the active site with possible steric interactions between substrate molecules modifying reaction rates (Lin et al., 2001; Torimoto et al., 2003). Indeed non-M-M kinetics have been rationalised on the basis of simultaneous binding of multiple ligands within active sites (Atkins, 2005). CYPs with large-enough active sites relative to their substrates, would likely figure in such interactions and include CYPs 3A4 and 2C8 (Ma et al., 2017).

CYP2C8 is a CYP2C subfamily member that metabolises about 5% of therapeutic drugs (Rendic and Guengerich, 2015) with most of the substrates possessing an anionic moiety (Totah and Rettie, 2005). The first crystal structure of CYP2C8 showed a relatively large active site (Schoch et al., 2004) and additional crystal structures of the enzyme bound to different substrates showed the active site to be T- or Y- shaped (reviewed by (Gay et al., 2010). The size and shape of the CYP2C8 structure seem to allow compounds to adopt different orientations that can impact the rate of metabolism (Ma et al., 2017). Additionally, more than one molecule of a compound can fit in the active site (Schoch et al., 2008) making it possible for interactions involving molecules of the same substrate to modify reaction rates. AZD9496 (Fig 1A) is an oral non-steroidal selective estrogen receptor (ER) degrader (SERD) currently in clinical development for treatment of ER-positive breast cancer (De Savi et al., 2015; Weir et al., 2016). A Phase 1 study showed AZD9496 to be metabolised to two main metabolites M3 and M5 (Fig 1B) detected in plasma (Hamilton et al., 2018). The area under the concentration-time curve (AUC) of AZD9496 increased in reasonable proportion to increasing AZD9496 following single doses from 20 to 400mg. However, a more than dose-proportional increase in AUC and C_{max} was observed following a single dose of 600 mg. The more than dose-proportional increase in AUC at the single 600 mg dose was diminished after multiple doses that correlated with an over-proportional increase in the 4 β -

DMD # 81539

hydroxycholesterol to cholesterol ratio. The possible contribution of substrate inhibition to the dose non-linear pharmacokinetics of AZD9496 was therefore, investigated in this study.

In contrast to previous reports on substrate inhibition of CYPs being partial (Lin et al., 2001), complete substrate inhibition of CYP2C8 by AZD9496 was observed *in vitro*. Modelling of the inhibition kinetics suggested a mechanism that involves binding of at least two molecules of AZD9496 to an inhibitor site. Additionally, amodiaquine deethylation, a high affinity probe of CYP2C8 activity *in vitro* (Li et al., 2002) was used to confirm the completeness of the inhibition.

Materials and Methods

Chemicals and reagents

AZD9496 and its metabolites M3 and M5 (Fig 1B) were synthesised in-house at AstraZeneca (De Savi et al., 2015). Amodiaquine hydrochloride, desethylamodiaquine, reduced nicotinamide adenine dinucleotide phosphate (NADPH) and rifampicin were purchased from Sigma-Aldrich (Poole, UK). Cryopreserved human hepatocytes, pool of 10 male and female donors were purchased from Bioreclamation IVT (Baltimore, MD, USA). Pooled human liver microsomes (HLM), ultra-pool of 150 male and female donors (catalog No. 452117), was obtained from Corning (Woburn MA, USA). Male and female individual donor HLMS were obtained from Corning (Woburn MA, USA). Recombinant CYP2C8 and control insect cell microsomes were purchased from Corning (Woburn MA, USA). All rCYPs were obtained from Corning (Woburn MA, USA). Methanol and acetonitrile were obtained from Thermo Fisher Scientific (Hemel Hempstead, UK). Lebovitz media was purchased from Life Technologies (Hemel Hempstead, UK). Cryopreserved HepaRG cells, HepaRG media supplements, CYP2C8-specific primer and probe mix, Dulbecco's Phosphate-buffered Saline and Williams' Media E were purchased from Thermo Fisher Scientific (Carlsbad, CA, USA). Fastlane Cell Multiplex NR kit was purchased from Qiagen (Manchester, UK). GAPDH-specific primer and probe mix was purchased from Eurogentec (Liege, Belgium).

Incubation conditions for recombinant human CYPs and HLM

The reaction mixture consisted of the appropriate amount of enzyme, potassium phosphate buffer pH 7.4 (final concentration 0.1 M), NADPH (final concentration 1 mM), appropriate concentration of compound (AZD9496 or amodiaquine). After a pre-incubation period of 5 minutes at 37°C, the reaction was started by adding NADPH followed by incubation for the appropriate time. The reaction was stopped using ice-cold acetonitrile (100%, v/v) containing

DMD # 81539

a different AZ compound as internal standard. The mixture was centrifuged at 3000 x g, 4°C for 10 minutes and the supernatant was transferred to a clean 96-well plate for injection into the mass spectrometer.

Substrate inhibition kinetics

Linearity of formation of the metabolites M3 and M5 was established with respect to protein concentration (HLM and r CYP2C8) and time. The incubation times were 20 and 30 minutes for HLM and rCYP2C8, respectively. The reaction rate with increasing concentrations of AZD9496 (0.05 to 200 µM) was determined as described above (incubation conditions for recombinant human CYPs and HLM). Standard curves were prepared by adding known concentrations (5 nM – 1000 nM) of M3 and M5 to reaction mixtures (without AZD9496 or NADPH) and the samples were processed for analysis by mass spectrometry as stated above.

Recombinant human CYP screen for formation of M3 and M5

A total of nine recombinant human CYP isoforms were screened for their contribution to formation of the major metabolites of AZD9496, M3 and M5. Each rCYP (20 pmols) was incubated with 2 µM of AZD9496 for 25 min at 37°C. No standard curves were prepared and the amounts of M3 and M5 formed were expressed as the ratio of peak area of metabolite/peak area of internal standard.

Effect of AZD9496 on amodiaquine deethylation

The effect of AZD9496 on amodiaquine deethylation was determined by adding AZD9496 (final concentration 100 µM) and amodiaquine (final concentration 50 µM) to the reaction mixture. Control experiments were included in which NADPH was added after stopping the reaction using ice-cold acetonitrile containing internal standard. The amount of

DMD # 81539

desethylamodiaquine was quantified as the response ratio (peak area of desethylamodiaquine: peak area of internal standard).

Intrinsic clearance of AZD9496 and amodiaquine

Amodiaquine and AZD9496 were incubated separately at a final concentration of 1 μ M with human liver microsomes from 8 different donors (final concentration of 1 mg/ml HLM). The reaction was started by adding NADPH and aliquots were taken at 0, 2, 4, 6, 8 and 10 minutes for amodiaquine and at 0, 5, 10, 20, 40 and 60 minutes for AZD9496 and added to acetonitrile (100% v/v, containing internal standard). The amount of amodiaquine or AZD9496 remaining (peak area: peak area of internal standard) at each time point was calculated as a percentage of the amount at the zero time point and the intrinsic clearance (CL_{int}) was determined as described previously (Obach et al., 1997).

Metabolism of AZD9496 by human hepatocytes

Cryopreserved human hepatocytes (Bioreclamation IVT, Baltimore, MA, USA) were rapidly thawed in a 37°C water bath and added to pre-warmed Leibovitz media. After gentle mixing, the cell suspension was centrifuged at 40 x g for 4 min at room temperature. After removing excess media, the cells were resuspended in about 5 ml of media. An aliquot (100 μ l) of the cell suspension was added to trypan blue (0.1 % v/v) solution and the mixture was used for manual counting of cells using the improved Neubauer counting chamber. Cells with greater than 80% viability were used. Cells (247.5 μ l) were added to a 96-well plate and pre-warmed to 37°C on a Hamilton Robot. The reaction was started by adding AZD9496 (2.5 μ l) to achieve final concentrations (0-200 μ M). The final concentration of organic solvent was 0.75%. An aliquot was taken after a 20 minutes incubation and added to acetonitrile (100%

DMD # 81539

v/v, containing internal standard). After centrifugation, the supernatant was injected into the mass spectrometer.

Non-specific Binding of AZD9496 to human liver microsomes

Non-specific binding of AZD9496 to human liver microsomes was assessed using the rapid equilibrium dialysis 96-well kit from Thermo Fisher Scientific (Rockford, IL, USA).

AZD9496 (at different concentrations covering those used for determining kinetic constants) was mixed with the appropriate concentration of human liver microsomes (0.025, 0.25 or 1 mg/ml) and potassium phosphate buffer (0.1 M, pH 7.4). The mixture was dialysed against buffer (potassium phosphate 0.1 M, pH 7.4) at 37°C with shaking for 4 hours. An equal volume was taken from the buffer-only and human liver microsomal-containing chambers. A corresponding volume of human microsomal mixture was added to the buffer-only sample and similarly, a corresponding volume of buffer was added to the sample taken from the human liver microsomal-containing chamber. After adding acetonitrile (100% containing internal standard), the mixture was vortex-mixed and centrifuged at 3000 xg for 10 min. The supernatant was transferred to a fresh 96-well plate and 3 µl was injected into the mass spectrometer. The concentration of compound was calculated as the ratio of the peak area of compound: peak area of internal standard. The percentage free was calculated as (the concentration in buffer chamber/concentration in HLM chamber) x 100%.

Effect of AZD9496 on CYP2C8 mRNA in HepaRG cells

Cryopreserved HepaRG cells were thawed and plated at a density of 100,000 viable cells per well in collagen 1 coated 96-well plates as per manufacturer's instructions. Approximately 72 hours after seeding cells were incubated with 0.0091 – 20 µM AZD9496 or rifampicin (positive control inducer) or vehicle control for 48 hours, with compound solutions replaced

DMD # 81539

after 24 hours. All compound solutions were prepared in Williams' Media E with serum-free induction supplement and a final concentration of 0.1% DMSO. After 48 hours treatment, cells were washed with Dulbecco's phosphate buffered saline and then assessed for induction of CYP mRNA. mRNA was prepared from the plated cells according to the FastLane Cell Multiplex NR kit protocol and relative expression levels evaluated by quantitative RT-PCR using CYP2C8 specific primers and probes and GAPDH as a housekeeping gene. Fold induction of CYP2C8 mRNA was calculated for each well relative to vehicle control wells and plotted against test item concentration.

Liquid chromatography with mass spectrometric detection

Chromatography of AZD9496 and its two metabolites was performed on a Waters Acquity UPLC pump (Waters, Milford, MA, USA) fitted with a C-18 Kinetex column (50 x 2.1 ID, 2.6 μ m) maintained at a temperature of 50°C with A) 0.1% formic acid in water and B) 0.1% formic acid in methanol (100%, v/v) as mobile phases. The gradient elution program at a flow rate of 0.6 ml/min started with 95% A for 1.5 minutes, a decrease to 25% in 3.3 minutes, held at 25% for 0.5 minutes, back to 95% in 0.1 minutes and held for 0.1 minutes to give a total run time of 5.5 minutes. Mass spectrometric detection was done in positive mode on the Waters TQD (Waters, Milford, MA) with data acquisition done using MassLynx V4.1. The gas flow was set at 600 L/hour (desolvation) and 50 L/hour (cone). The desolvation and source temperatures were set at 350 and 120°C, respectively. The capillary voltage was 3.27kV and the analytes were monitored by multiple reaction monitoring with the details of the scan parameters shown in Table 1.

DMD # 81539

Chromatography of amodiaquine and its metabolite desethylamodiaquine, was also performed on a Waters Acquity UPLC pump fitted with a C-18 Kinetex column (50 x 2.1 ID, 2.6 μ m) maintained at a temperature of 50°C with A) 0.1% formic acid in water and B) 0.1% formic acid in methanol (100%, v/v) as mobile phases. The gradient elution program at a flow rate of 0.6 ml/minute started with 95% A for 0.3 minutes, a decrease to 5% in 2.5 minutes, held at 5% for 0.2 minutes, back to 95% in 0.2 minutes and held for 0.3 minutes to give a total run time of 3.5 minutes. Mass spectrometric detection was done in positive mode on the Waters Xevo TQS (Waters, Milford, MA, USA) with data acquisition done using MassLynx V4.1 (Waters, Milford, MA, USA). The capillary voltage was set at 0.71kV and desolvation temperature was set at 600°C. Gas flows were set at: desolvation (1000 L/hour) and cone (150 L/hour). Amodiaquine and desethylamodiaquine were monitored by multiple reaction monitoring at cone and collision voltages of 20 and 22, respectively. The transitions for amodiaquine were 356.5 > 284.5 and for desethylamodiaquine, 328.6 > 283.4.

Data and statistical analysis

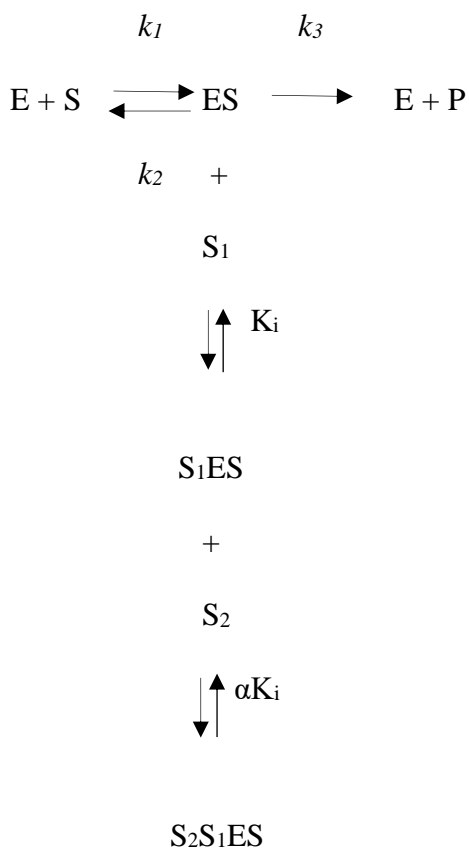
The inhibition data generated in this study was fitted to the generally accepted model for substrate inhibition analogous to uncompetitive inhibition (Yoshino and Murakami, 2015) (model (1)) in GraphPad Prism Version 7.02 (GraphPad Software Inc., La Jolla, CA, USA).

$$V = V_{\max}/(K_m + [S](1 + [S]/K_i)) \quad 1.$$

New models of substrate inhibition essentially similar to model 1 with the exception of an additional substrate molecule, added to try and explain the greater extent of inhibition that model 1 failed to describe were considered. The binding of an additional two molecules (forming an S_1S_2ES complex) was assumed taking into account proposals by others (Korzekwa et al., 1998) in which some atypical reactions may involve binding of two

DMD # 81539

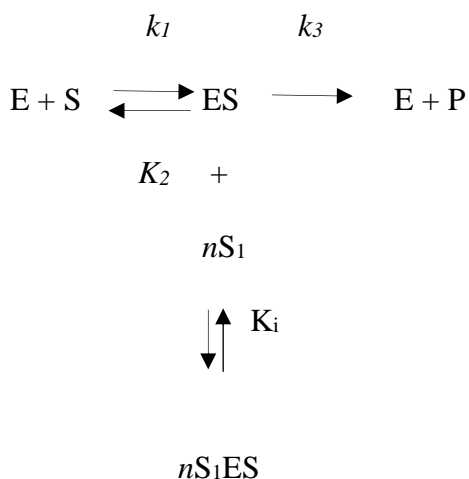
substrate molecules and an effector molecule. Model (2) assumed sequential binding of two molecules with the first facilitating binding of the second as shown below.



This gives the equation (2):

$$V = V_{\max}[\text{S}]/(K_m + [\text{S}](1 + [\text{S}]/k_i + [\text{S}]^2/\alpha k_i^2)) \quad 2.$$

The third model assumed simultaneous binding of n (number determined from the data) molecules of AZD9496 to the inhibitor site as shown below.



DMD # 81539

$$V = V_{\max}/(K_m + [S](1 + [S]^n/K_i^n) \quad 3.$$

Equations (2) and (3) were imported into GraphPad Prism and were tested for their ability to describe the inhibition data in this study. Comparison of the models was done in GraphPad Prism using the extra-sum-of-squares F test. An F ratio around 1 shows the simpler model (1) to be the correct one but a ratio much greater than 1 supports use of the more complicated one. A p value can then be used to show statistical significance – a p value less than 0.05 shows that the simpler model (less parameters and in this study, equation 1) is incorrect. The data and statistical analysis comply with the recommendations on experimental design and analysis in pharmacology (Motulsky and Christopoulos, 2004).

Concentration of AZD9496 available to interact with enzymes *in vivo*

The free concentration of AZD9496 likely to interact with enzymes *in vivo* after administration of a 600 mg dose was estimated according to (Ito et al., 1998; Ito et al., 2002; Rostami-Hodjegan and Tucker, 2004) assuming complete solubility and bioavailability. The maximum intestinal concentration = molar dose/250 ml, the maximum liver inlet concentration, $I_{in\ max} = F_a \cdot K_a \cdot \text{Dose}/Q_h$, $I_{in\ free} = I_{in\ max} \cdot fu$. I = total C_{\max} and F_a is the fraction absorbed and this was assumed to be 1. K_a is the absorption rate constant which was assumed to be $0.1\ min^{-1}$. Q_h is the hepatic blood flow (1500 ml/minute). A blood to plasma ratio of 0.66 (experimentally determined) was used and for the fraction unbound FDA guidance value of 0.01 (FDA, 2017) for highly bound compounds was applied.

Results

Metabolism of AZD9496 by human liver microsomes

The HLM protein concentrations and time that gave linear formation of the metabolites of AZD9496 were established. The effect of increasing concentrations of AZD9496 on the rate of metabolism in HLM was investigated using 0.025 and 0.25 mg/ml of HLM protein for 20 min. At both 0.025 mg/ml and 0.25 mg/ml HLM protein, the rate of formation of the major metabolite M3 showed complete substrate inhibition (Fig 2A and 2B) that is the rate of formation of the metabolite went down to zero at 200 μ M of AZD9496. The minor metabolite M5 also showed a similar pattern of substrate inhibition.

The data for formation of the major metabolite (M3) fitted poorly to the generally accepted model of substrate inhibition analogous to uncompetitive inhibition (model 1) and the poor fit was more pronounced when less enzyme (0.025 mg/ml HLM protein) was used (Fig 2A and 2B). Two additional models to the generally accepted substrate inhibition model were used to fit the data as described in the materials and methods. Fitting the inhibition data to the second model (2) gave visually better fits, however, these were deemed ambiguous by the program and did not generate kinetic parameters. Model (3) was a modification of model (1) that did not have any constraints on the number of [S] that could bind to the inhibitor site i.e. while [S] is equal to one in model (1), this value was determined from the data by the program for model (3). Modelling the data using equation (3) gave much better fits (Fig 2C and 2D). In addition, the two models were compared using the extra-sum-of-squares F test. The F ratios obtained were 22 ($P < 0.0001$) and 10 ($P = 0.0034$) for 0.025 mg/ml and 0.25 mg/ml HLM, respectively. The enzyme kinetic parameters obtained using models (1) and (3) are shown in table 2 with K_m and K_i values corrected for protein binding which is described below.

DMD # 81539

Non-specific protein binding

The non-specific binding of AZD9496 to HLM in vitro was assessed using rapid equilibrium dialysis at three different HLM concentrations of 0.025, 0.25 and 1 mg/ml. The percentage of AZD9496 non-specifically bound to HLM increased with increase in HLM protein concentration. At least 91% of AZD9496 was non-specifically bound to HLM matrix at the highest HLM concentration of 1 mg/ml (Fig 3). At the four concentrations of AZD9496 tested (0.5-200 μ M), there did not seem to be a significant difference in the extent of nonspecific binding at each HLM concentration except at the 1.0 mg/ml HLM concentration where 200 μ M AZD9496 seems to result in a higher percentage of free drug (16% compared to about 7% at the other concentrations).

CYP identification

A total of nine recombinant human CYP isoforms were screened for their contribution to formation of the main metabolites of AZD9496, M3 and M5. The concentrations of M3 and M5 were expressed as the response ratio (peak area of metabolite: peak area of internal standard). M3 and M5 were detected in incubations containing CYP2C8 only (Fig 4A). In order to confirm CYP2C8 as the major isoform responsible for metabolism of AZD9496, a correlation analysis of the intrinsic clearance (CL_{int}) of AZD9496 and the CYP2C8-specific probe amodiaquine was done in human liver microsomes HLM from eight different donors. A good correlation ($r^2 = 0.78$) was observed between CL_{int} values for AZD9496 and amodiaquine (Fig 4B).

Completeness of substrate inhibition

To check the completeness of the substrate inhibition and to rule out the possibility of AZD9496-specific artefacts, the impact of AZD9496 on the formation of desethylamodiaquine from amodiaquine in HLM was assessed. The concentration of amodiaquine used (50 μ M) while AZD9496 was incubated at 100 μ M (the same concentration that inhibited 100% of M3 formation at 0.025 mg/ml of HLM protein. The amount of desethylamodiaquine formed was quantified by measuring the peak area to internal standard ratio and this was expressed as a percentage with the amodiaquine only incubation set at 100%. The control incubations for amodiaquine only and amodiaquine plus AZD9496 had NADPH (the cofactor required by CYPs) added to them after stopping the reaction. These were compared to the reactions in which NADPH was present at the start. The controls had similar levels of desethylamodiaquine as the AZD9496 plus amodiaquine incubation showing that AZD9496 caused complete inhibition of desethylamodiaquine formation (Fig 5).

Significance of the value of n

Given the different numbers of n (number of AZD9496 molecules bound to the inhibitor site) predicted by GraphPad Prism under different conditions (protein concentration), the effect of enzyme concentration on the value of n was studied using recombinant CYP2C8 (0.4 pmols and 4 pmols). Given the extensive non-specific protein binding of AZD9496, the protein concentration was kept constant by adding control baculovirus microsomes (heterologous expression system used to produce the recombinant human CYP2C8 used in this study). The number of AZD9496 molecules predicted to bind to the inhibitor site was 2-fold higher when less enzyme was used (Fig 6A and 6B). The K_m values were the same (0.67 μ M) but the K_i value was higher when less enzyme was used (14 compared to 6 μ M).

DMD # 81539

Confirmation of substrate inhibition in human hepatocytes

Human hepatocytes were used to assess whether the substrate inhibition exhibited by AZD9496 in HLM and rCYP2C8 was not a microsomal artefact. Human hepatocytes at 0.125 and 1 million cells/ml were incubated with increasing concentrations of AZD9496. A profile of substrate inhibition similar to that in HLM and recombinant CYP2C8 was observed in hepatocytes with almost complete inhibition observed when less cells were used (Fig 7A and 7B). Multiple AZD9496 molecules may also bind to the enzymes in hepatocytes as shown by n values of 2.2 and 3 for 0.125 and 1 million cells/ml, respectively. Similar K_m values of 7.8 and 8.7 μM were observed.

Induction of CYP2C8 mRNA in HepaRG cells

Plated HepaRG cells were used to assess whether AZD9496 induced CYP2C8 mRNA (Fig 8). The magnitude of CYP2C8 mRNA induction in plated HepaRG cells was observed to be small, with the positive control inducer rifampicin demonstrating a calculated E_{max} of 1.8 ± 0.13 fold. AZD9496 also demonstrated a concentration dependent induction of CYP2C8 mRNA to a maximum at 20 μM that was 155% of the rifampicin control.

Free AZD9496 concentrations achieved after administration of a single 600 mg dose

After administration of a single 600 mg dose of AZD9496, the total plasma C_{max} was 17.9 μM (Hamilton et al., 2018). This gave a predicted intestinal concentration of 5424 μM , $I_{\text{in max}}$ of 102 μM . The $I_{\text{in free}}$, estimated using the FDA guidance for highly bound compounds (f_u of 0.01) was 1.0 μM .

Discussion

Substrate inhibition is a common mechanism of enzyme inhibition however, many questions have been raised concerning its relevance. Indeed some have dismissed it as an *in vitro* artefact (Reed et al., 2010) as the majority of cases of substrate inhibition occur at very high substrate concentrations that would almost never be achieved *in vivo* (Lin et al., 2001). In addition to an *in vitro* microsomal system, others have suggested the use of other systems such as hepatocytes to confirm any observed substrate inhibition (Houston and Galetin, 2005). In this study, HLM, recombinant human CYP2C8 and human hepatocytes were used to show a similar profile of complete substrate inhibition of CYP2C8 by the oral selective estrogen receptor degrader (SERD) AZD9496. In addition, the completeness of the inhibition was demonstrated using the specific probe of CYP2C8 activity amodiaquine deethylation.

The substrate inhibition observed with AZD9496 did not conform to the generally accepted model analogous to uncompetitive inhibition, model (1) (Yoshino & Mukarami, 2015) with the data showing a greater degree of inhibition than could be described by the model. Additionally, visual inspection of the data and kinetic parameters showed that this was not the correct model to use - the V_{\max} values were much higher than was suggested by the data. Mathematically, one of the ways in which the greater degree of inhibition could be accounted for was an increase in the number of substrate molecules causing the inhibition i.e. increasing the value of [S] in the denominator of equation 1. The fitting of two or more substrate molecules in the active site that could theoretically include an inhibitory site, is supported by the large volume of the CYP2C8 active site (Schoch et al., 2004). Additional support for multiple substrate binding comes from studies by others which show that a substrate can adopt multiple binding orientations within the CYP2C8 active site (Kerdpin et al., 2004). It is therefore, possible for at least two molecules of AZD9496 to bind to the active site of

DMD # 81539

CYP2C8 in productive and non-productive orientations. Inhibition of the enzyme could theoretically occur because of a molecule bound in a non-productive orientation interfering with the productive binding thus reducing the rate of reaction or preventing the product from leaving the active site.

Model (2) was derived based on the binding of two substrate molecules to an inhibitor site with the first molecule facilitating binding of the next (equation 2). Visually, the model gave a better fit compared to the generally accepted one (1), however, the program could not give values of the parameters as this was deemed an ambiguous fit. The generally accepted model (1) was modified to give model (3) by removing any constraints on the number of AZD9496 molecules occupying the inhibitor site with the number of [S] determined by the inhibition data. Notably, model (3) gave the best fits of the data by assigning different numbers of molecules bound to the inhibitory site based on the data. In addition, comparison of the two models using the sum-of-squares F test and associated p values showed model 3 to be the better model. The number (n) of molecules of AZD9496 predicted to interact with the inhibitor site differed depending on the amount of protein used and this was investigated further.

AZD9496 is extensively non-specifically bound to protein *in vitro*. Using different amounts of protein in incubations would in turn mean different concentrations of AZD9496 available to interact with the enzyme. There was up to a 10-fold difference in percentage free AZD9496 at 0.025 mg/ml compared to 1 mg/ml HLM protein. In addition, the difference in protein concentration would also mean a difference in the amount of enzyme. Given that the impact of protein concentration was straightforward, i.e. it reduced the concentration of AZD9496 available to interact with the enzyme, we investigated the impact of different

enzyme concentrations on the enzyme kinetics using recombinant CYP2C8 (at 0.4 pmols and 4 pmols). Microsomes from control insect baculovirus (the heterologous expression system of the human recombinant CYP2C8 utilised in the study) were used to maintain the same protein concentration in both 0.4 and 4 pmols arms of the experiment. Interestingly, the number of molecules of AZD9496 predicted to bind to the inhibitor site were higher when less enzyme was used. The higher K_i value associated with less enzyme might seem counter-intuitive but may simply reflect the binding of twice the number of AZD9496 molecules and is not an indicator of the strength of binding when comparing the two protein concentrations. The greater degree of inhibition when less enzyme is used likely comes from a “removal” of the extra molecule through binding to the inhibitor site instead of contributing to the increased rate of product formation that would occur when a higher concentration of enzyme is used. Our hypothesis is that AZD9496 initially binds to the active site in a productive orientation with involvement of an inhibitory site occurring as more substrate becomes available. A high $[S]:[E]$ ratio allows for the maximum number of AZD9496 molecules to occupy the inhibitor site and is supported by the higher K_i values compared to K_m values.

The possible *in vivo* relevance of the complete substrate inhibition observed in this study is intriguing. The potential for dose nonlinearity from typical M-M kinetics can be assessed by comparing the K_m value to the expected *in vivo* free drug concentrations (Ludden, 1991). A lower K_m value compared to drug concentrations would lead to saturation of metabolism and dose non-linearity. Another possible cause of dose-nonlinearity is time-dependent inhibition, however, AZD9496 did not inhibit CYP2C8 in a time-dependent manner (data not shown). For complete substrate inhibition, an increase in concentration of substrate would be expected to result in an increase in the percentage inhibition of its own metabolism across all concentrations up to V_{max} . Each increase in dose would therefore, be expected to result in a

DMD # 81539

higher than linear exposure with the greatest nonlinear exposure occurring at concentrations where the rate of product formation goes down to zero. Added to this is the possible impact of the amount of CYP2C8 enzyme an individual has on the extent of inhibition with individuals expressing highest protein likely to experience the least amount of inhibition. A wide range in extent of inhibition by AZD9496 is, therefore, expected as CYP2C8 is polymorphic and has been shown to exhibit high interindividual variation in protein expression of up to 33-fold (Naraharisetti et al., 2010). In the phase 1 study by (Hamilton et al., 2018), single doses of AZD9496 from 20 mg to 400 mg exhibited reasonably proportional increases in AUC and C_{max} . However, a more than dose-proportional increase in AUC and C_{max} was observed after administration of the highest single dose (600 mg on day 1). After the single 600 mg dose, the maximum unbound liver inlet concentration was estimated to be 1 μ M which would be higher than the K_m of 0.4 μ M (in HLM) for CYP2C8. The extent of substrate inhibition likely to occur at this dose is not clear but could explain the apparent dose-nonlinearity. While formation of M3 and M5 was mediated mainly by CYP2C8, depletion of AZD9496 was observed in incubations with CYP3A4 and CYP3A5 (data not shown). Upon multiple 600 mg twice daily dosing, the observed more-than dose proportional decrease in AUC on day 15 vs day 1 would be consistent with induction of CYP3A and CYP2C8 at these concentrations.

In conclusion and in contrast to previous reports (Lin et al., 2001), substrate inhibition of CYP2C8 by AZD9496 was shown to be complete and not just partial. The inhibition likely involves binding of at least two molecules of AZD9496 to the inhibitor site which may be in the active site of the enzyme. Given that CYP2C8 is the major isoform catalysing formation of the two major metabolites of AZD9496, our results suggest substrate inhibition as the

DMD # 81539

cause of the observed dose non-linearity at the highest single dose of AZD9496 tested in the clinic (i.e. 600 mg).

DMD # 81539

Acknowledgements

We thank Dr. Dermot McGinnity for useful discussions.

Authorship contributions

Participated in research design: Bapiro, Sykes and Jones.

Conducted the experiments: Bapiro, Rollison

Performed data analysis: Bapiro, Sykes, Martin, Davies, Yates, Hoch, Rollison, Jones

Wrote or contributed to the writing of the manuscript: Bapiro, Sykes, Martin, Davies, Yates, Hoch, Rollison, Jones.

References

- Atkins WM (2005) Non-Michaelis-Menten kinetics in cytochrome P450-catalyzed reactions. *Annu Rev Pharmacol Toxicol* **45**:291-310.
- De Savi C, Bradbury RH, Rabow AA, Norman RA, de Almeida C, Andrews DM, Ballard P, Buttar D, Callis RJ, Currie GS, Curwen JO, Davies CD, Donald CS, Feron LJ, Gingell H, Glossop SC, Hayter BR, Hussain S, Karoutchi G, Lamont SG, MacFaul P, Moss TA, Pearson SE, Tonge M, Walker GE, Weir HM, and Wilson Z (2015) Optimization of a Novel Binding Motif to (E)-3-(3,5-Difluoro-4-((1R,3R)-2-(2-fluoro-2-methylpropyl)-3-methyl-2,3,4,9-tetra hydro-1H-pyrido[3,4-b]indol-1-yl)phenyl)acrylic Acid (AZD9496), a Potent and Orally Bioavailable Selective Estrogen Receptor Downregulator and Antagonist. *J Med Chem* **58**:8128-8140.
- FDA (2017) In Vitro Metabolism- and Transporter-Mediated Drug-Drug Interaction Studies Guidance for Industry.
- Gay SC, Roberts AG, and Halpert JR (2010) Structural features of cytochromes P450 and ligands that affect drug metabolism as revealed by X-ray crystallography and NMR. *Future Med Chem* **2**:1451-1468.
- Hamilton EP, Patel MR, Armstrong AC, Baird RD, Jhaveri K, Hoch M, Klinowska T, Lindemann JPO, Morgan S, Schiavon G, Weir HM, and Im SA (2018) A first in human study of the new oral selective estrogen receptor degrader AZD9496 for HR+/HER2- advanced breast cancer. *Clin Cancer Res*.
- Houston JB (1994) Relevance of in vitro kinetic parameters to in vivo metabolism of xenobiotics. *Toxicol In Vitro* **8**:507-512.
- Houston JB and Galetin A (2005) Modelling atypical CYP3A4 kinetics: principles and pragmatism. *Arch Biochem Biophys* **433**:351-360.
- Ito K, Chiba K, Horikawa M, Ishigami M, Mizuno N, Aoki J, Gotoh Y, Iwatsubo T, Kanamitsu S, Kato M, Kawahara I, Niinuma K, Nishino A, Sato N, Tsukamoto Y, Ueda K, Itoh T, and Sugiyama Y (2002) Which concentration of the inhibitor should be used to predict in vivo drug interactions from in vitro data? *AAPS PharmSci* **4**:E25.
- Ito K, Iwatsubo T, Kanamitsu S, Ueda K, Suzuki H, and Sugiyama Y (1998) Prediction of pharmacokinetic alterations caused by drug-drug interactions: metabolic interaction in the liver. *Pharmacol Rev* **50**:387-412.
- Kerdpin O, Elliot DJ, Boye SL, Birkett DJ, Yoovathaworn K, and Miners JO (2004) Differential contribution of active site residues in substrate recognition sites 1 and 5 to cytochrome P450 2C8 substrate selectivity and regioselectivity. *Biochemistry* **43**:7834-7842.
- Korzekwa KR, Krishnamachary N, Shou M, Ogai A, Parise RA, Rettie AE, Gonzalez FJ, and Tracy TS (1998) Evaluation of atypical cytochrome P450 kinetics with two-substrate models: evidence that multiple substrates can simultaneously bind to cytochrome P450 active sites. *Biochemistry* **37**:4137-4147.
- Li XQ, Bjorkman A, Andersson TB, Ridderstrom M, and Masimirembwa CM (2002) Amodiaquine clearance and its metabolism to N-desethylamodiaquine is mediated by CYP2C8: a new high affinity and turnover enzyme-specific probe substrate. *J Pharmacol Exp Ther* **300**:399-407.
- Lin Y, Lu P, Tang C, Mei Q, Sandig G, Rodrigues AD, Rushmore TH, and Shou M (2001) Substrate inhibition kinetics for cytochrome P450-catalyzed reactions. *Drug Metab Dispos* **29**:368-374.
- Ludden TM (1991) Nonlinear pharmacokinetics: clinical Implications. *Clin Pharmacokinet* **20**:429-446.
- Ma Y, Fu Y, Khojasteh SC, Dalvie D, and Zhang D (2017) Glucuronides as Potential Anionic Substrates of Human Cytochrome P450 2C8 (CYP2C8). *J Med Chem*.
- Motulsky H and Christopoulos A (2004) *Fitting models to biological data using linear and nonlinear regression. A practical guide to curve fitting.* . Oxford University Press, New York.
- Naraharisetti SB, Lin YS, Rieder MJ, Marciante KD, Psaty BM, Thummel KE, and Totah RA (2010) Human liver expression of CYP2C8: gender, age, and genotype effects. *Drug Metab Dispos* **38**:889-893.

DMD # 81539

- Obach RS, Baxter JG, Liston TE, Silber BM, Jones BC, MacIntyre F, Rance DJ, and Wastall P (1997) The prediction of human pharmacokinetic parameters from preclinical and in vitro metabolism data. *J Pharmacol Exp Ther* **283**:46-58.
- Obach RS and Reed-Hagen AE (2002) Measurement of Michaelis constants for cytochrome P450-mediated biotransformation reactions using a substrate depletion approach. *Drug Metab Dispos* **30**:831-837.
- Pelkonen O, Turpeinen M, Uusitalo J, Rautio A, and Raunio H (2005) Prediction of drug metabolism and interactions on the basis of in vitro investigations. *Basic Clin Pharmacol Toxicol* **96**:167-175.
- Reed MC, Lieb A, and Nijhout HF (2010) The biological significance of substrate inhibition: a mechanism with diverse functions. *Bioessays* **32**:422-429.
- Rendic S and Guengerich FP (2015) Survey of Human Oxidoreductases and Cytochrome P450 Enzymes Involved in the Metabolism of Xenobiotic and Natural Chemicals. *Chem Res Toxicol* **28**:38-42.
- Rostami-Hodjegan A and Tucker G (2004) 'In silico' simulations to assess the 'in vivo' consequences of 'in vitro' metabolic drug-drug interactions. *Drug Discov Today Technol* **1**:441-448.
- Schoch GA, Yano JK, Sansen S, Dansette PM, Stout CD, and Johnson EF (2008) Determinants of cytochrome P450 2C8 substrate binding: structures of complexes with montelukast, troglitazone, felodipine, and 9-cis-retinoic acid. *J Biol Chem* **283**:17227-17237.
- Schoch GA, Yano JK, Wester MR, Griffin KJ, Stout CD, and Johnson EF (2004) Structure of human microsomal cytochrome P450 2C8. Evidence for a peripheral fatty acid binding site. *J Biol Chem* **279**:9497-9503.
- Spracklin DK, Hankins DC, Fisher JM, Thummel KE, and Kharasch ED (1997) Cytochrome P450 2E1 is the principal catalyst of human oxidative halothane metabolism in vitro. *J Pharmacol Exp Ther* **281**:400-411.
- Tang C, Shou M, Mei Q, Rushmore TH, and Rodrigues AD (2000) Major role of human liver microsomal cytochrome P450 2C9 (CYP2C9) in the oxidative metabolism of celecoxib, a novel cyclooxygenase-II inhibitor. *J Pharmacol Exp Ther* **293**:453-459.
- Torimoto N, Ishii I, Hata M, Nakamura H, Imada H, Ariyoshi N, Ohmori S, Igarashi T, and Kitada M (2003) Direct interaction between substrates and endogenous steroids in the active site may change the activity of cytochrome P450 3A4. *Biochemistry* **42**:15068-15077.
- Totah RA and Rettie AE (2005) Cytochrome P450 2C8: substrates, inhibitors, pharmacogenetics, and clinical relevance. *Clin Pharmacol Ther* **77**:341-352.
- Venkatakrisnan K, Von Moltke LL, and Greenblatt DJ (2001) Human drug metabolism and the cytochromes P450: application and relevance of in vitro models. *J Clin Pharmacol* **41**:1149-1179.
- Weir HM, Bradbury RH, Lawson M, Rabow AA, Buttar D, Callis RJ, Curwen JO, de Almeida C, Ballard P, Hulse M, Donald CS, Feron LJ, Karoutchi G, MacFaul P, Moss T, Norman RA, Pearson SE, Tonge M, Davies G, Walker GE, Wilson Z, Rowlinson R, Powell S, Sadler C, Richmond G, Ladd B, Pazolli E, Mazzola AM, D'Cruz C, and De Savi C (2016) AZD9496: An Oral Estrogen Receptor Inhibitor That Blocks the Growth of ER-Positive and ESR1-Mutant Breast Tumors in Preclinical Models. *Cancer Res* **76**:3307-3318.
- Williams PA, Cosme J, Vinkovic DM, Ward A, Angove HC, Day PJ, Vonnrhein C, Tickle IJ, and Jhoti H (2004) Crystal structures of human cytochrome P450 3A4 bound to metyrapone and progesterone. *Science* **305**:683-686.
- Yoshino M and Murakami K (2015) Analysis of the substrate inhibition of complete and partial types. *Springerplus* **4**:292.

DMD # 81539

Footnotes

Financial support was provided by AstraZeneca.

Figure Legends

Figure 1.

The chemical structures of (A) AZD9496, its metabolites (B) M3 (the major metabolite) and M5 (minor metabolite) - a single structure has been used to represent the two metabolites as they are diastereoisomers but whose configuration is not known. The metabolite standards used in the study were, however, isomerically pure.

Figure 2.

The rate of formation of M3, the major metabolite of AZD9496 with increase in AZD9496 concentration in pooled human liver microsomes (HLM) at a concentration of A) 0.025 mg/ml and B) 0.25 mg/ml microsomal protein. Each point represents duplicate determinations and these were repeated on three separate occasions ($n = 3$). The data in Figs 2A and B were fit to the generally accepted substrate inhibition model (1). Figs 2C and D were fit using the new model in this study (model (3)). (C) is a fit of the data with 0.025 mg/ml HLM and (D) is 0.25 mg/ml HLM.

Figure 3.

The extent of non-specific binding of AZD9496 at different concentrations (0.5 – 200 μ M) to 3 different concentrations of HLM (0.025, 0.25 and 1 mg/ml) measured by rapid equilibrium dialysis. A single experiment was done at each concentration in triplicate.

Figure 4.

A screen for formation of the two main metabolites of AZD9496 in a panel of recombinant human CYPs (A). Incubations, in duplicate (with the average shown from a single experiment), were done using 20 pmols of enzyme and 2 μ M of AZD9496 for 25 minutes. (B) The relationship between AZD9496 and amodiaquine intrinsic clearance (CL_{int}) values

DMD # 81539

in human liver microsomes from eight different donors. The results are the average of duplicate determinations repeated on 3 separate occasions ($n = 3$).

Figure 5.

The effect of AZD9496 (100 μ M) on formation of desethylamodiaquine (measured as a percentage, with the amodiaquine only incubation set at 100%) after incubation of amodiaquine (50 μ M) with 0.025 mg/ml of human liver microsomes for 20 minutes. The reaction in the samples was started by adding NADPH while the controls had NADPH added after stopping the reaction with ice-cold acetonitrile. Each point represents the average of triplicate determinations and these were done on 3 separate occasions ($n=3$).

Figure 6.

Substrate inhibition of formation of the major metabolite (M3) of AZD9496 by recombinant human CYP2C8 (A) 0.4 pmols of CYP2C8 and (B) 4 pmols of CYP2C8. The protein concentrations in the 2 incubations were kept constant using control baculovirus microsomes. Each point represents duplicate determinations repeated on 3 separate occasions ($n = 3$).

Figure 7.

The substrate inhibition of formation of the main metabolite (M3) of AZD9496 by cryopreserved human hepatocytes (A) 0.125 million cells/ml and (B) 1 million cells/ml. The results are the average of duplicate determinations from a single experiment.

Figure 8

Fold induction of CYP2C8 mRNA in cultured HepaRG cells by AZD9496 and rifampicin. Each data point represents an individual determination in a single experiment.

DMD # 81539

Tables

Table 1. Mass spectrometry scan parameters

Analyte	Parent ion	Product ion	Cone (V)	Collision energy (V)
AZD9496	443.4	117.9	25	28
M3	459.4	133.8	30	18
M5	459.4	133.8	25	28

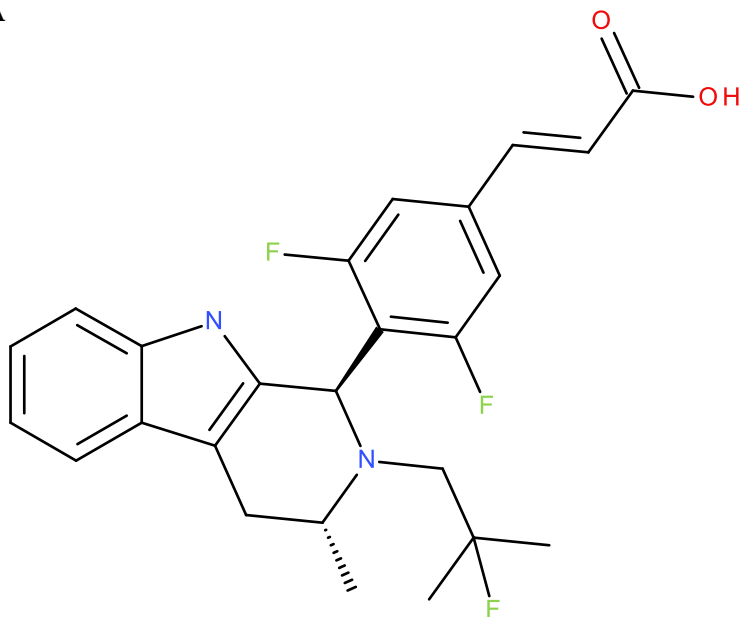
DMD # 81539

Table 2. Enzyme kinetic parameters (std error in parentheses) for AZD9496 in HLM with the different models

	Equation (1)	Equation (3)
HLM 0.025 mg/ml		
K_m (μM)	1.3 (1.0)	0.4 (0.2)
V_{\max} (pmol/min/mg)	194 (69)	93 (8.4)
Value of n	1	3 (0.8)
K_i (μM)	3.3 (2.2)	12 (1.4)
HLM 0.25 mg/ml		
K_m (μM)	2.5 (3.7)	0.8 (0.7)
V_{\max} (pmol/min/mg)	169 (68)	76 (12)
Value of n	1	1.8 (0.4)
K_i (μM)	2.3 (3.2)	8.1 (4.4)

Figure 1

A



B

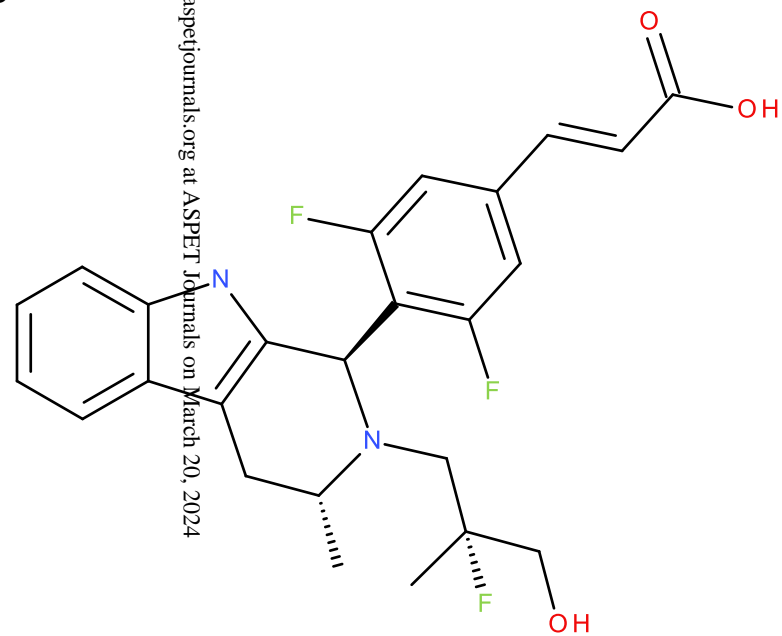


Figure 2

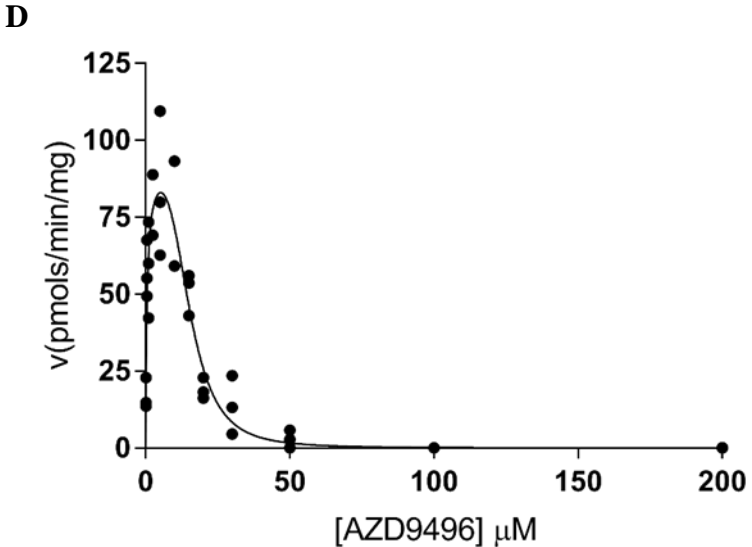
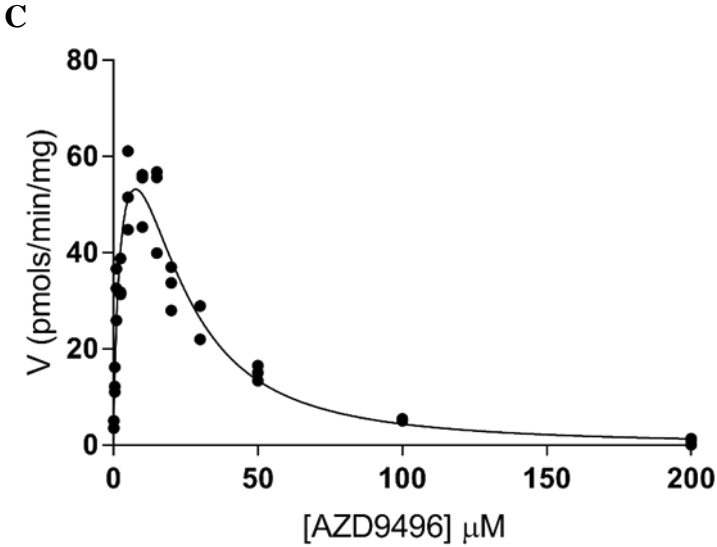
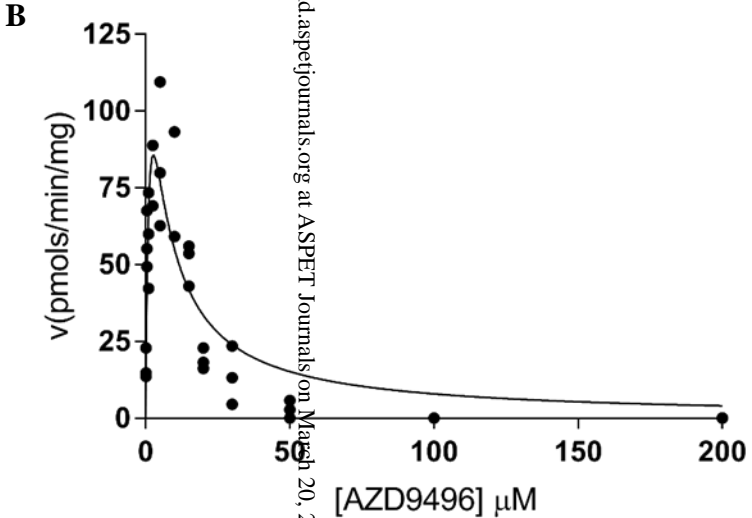
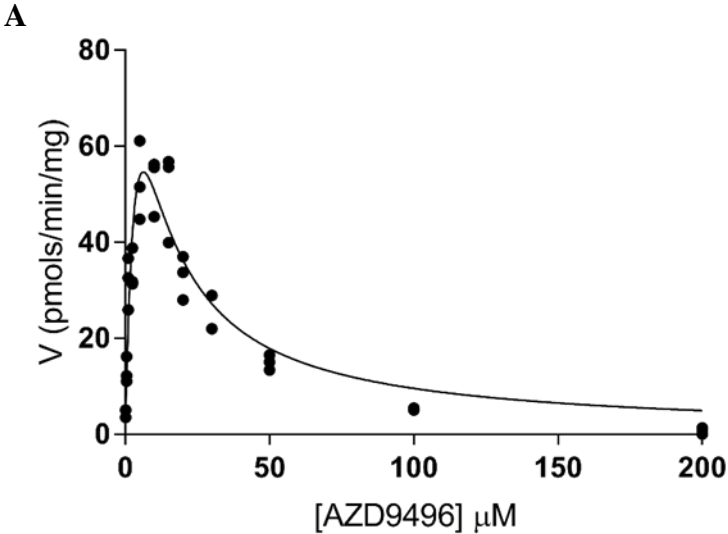


Figure 3

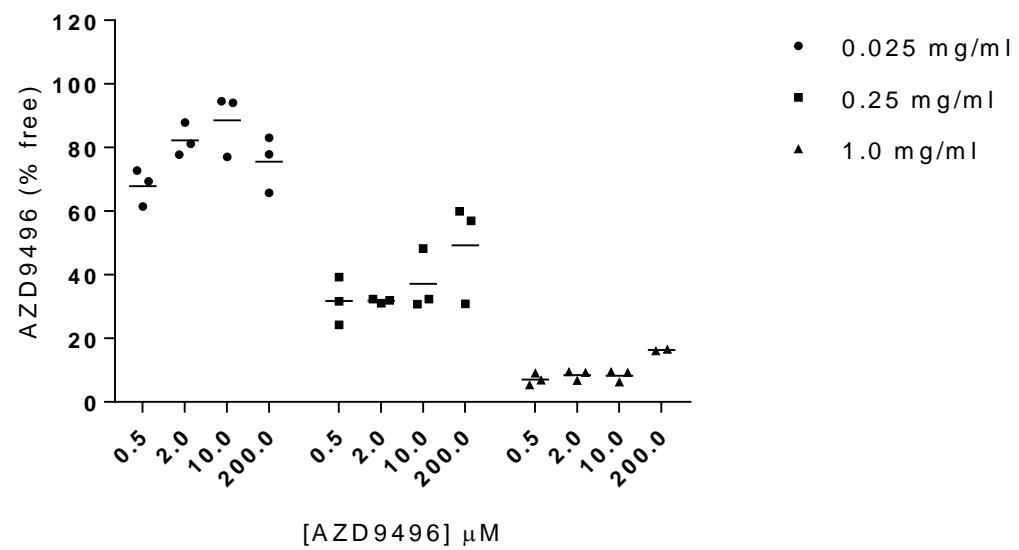
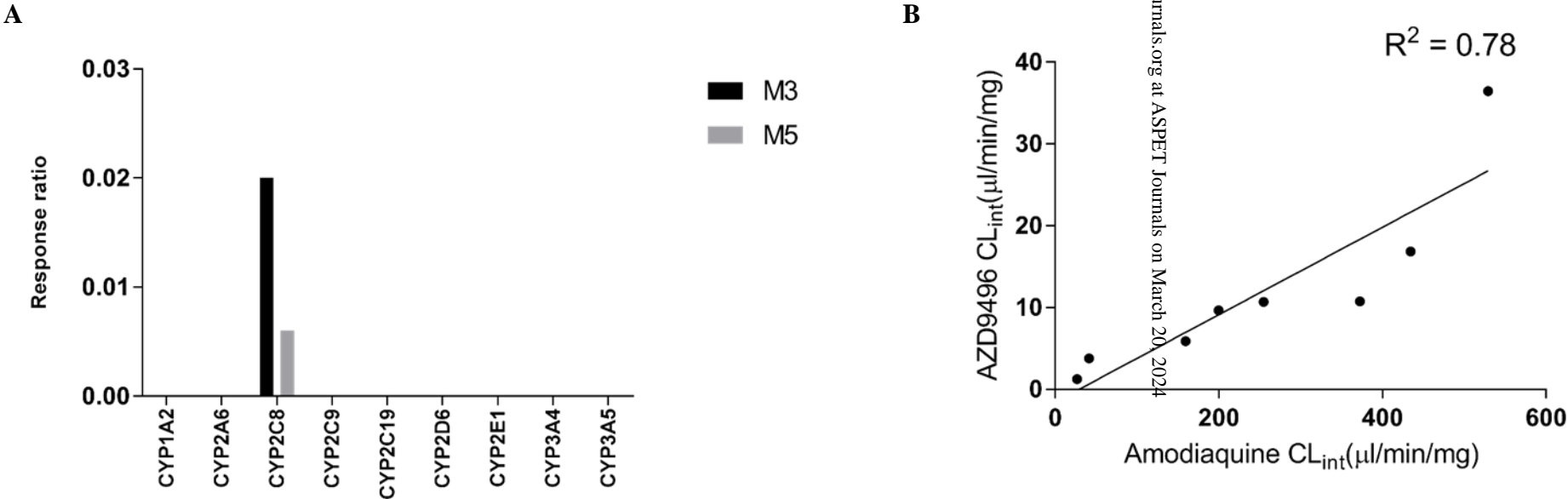


Figure 4



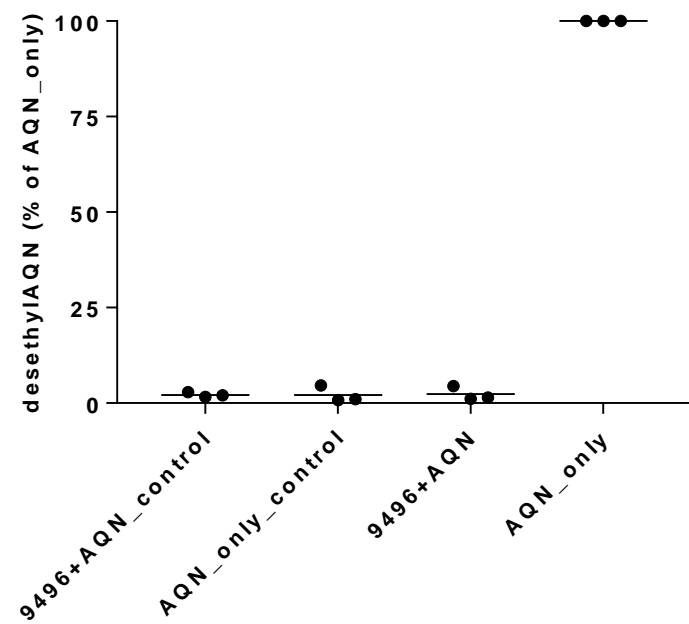
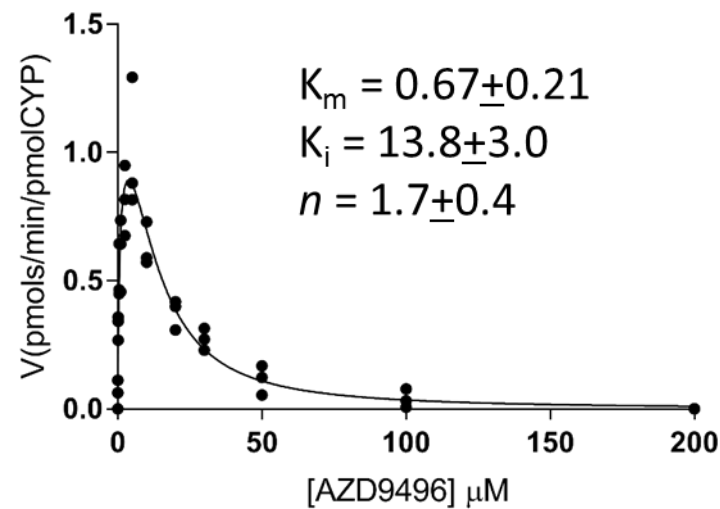


Figure 5

Figure 6

A



B

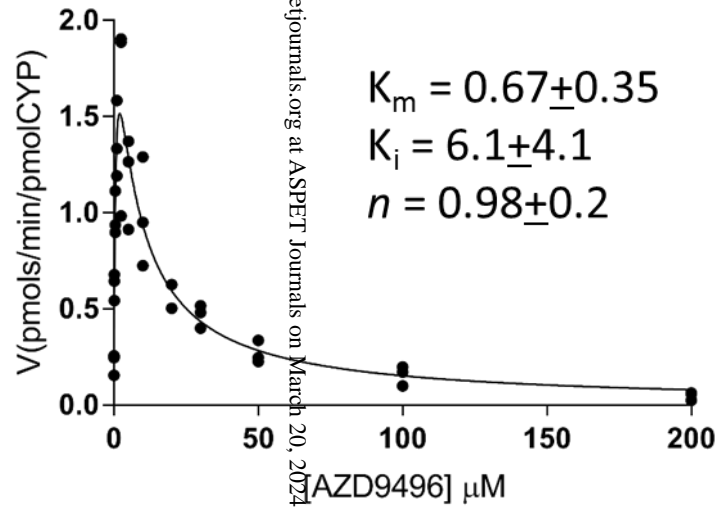


Figure 7

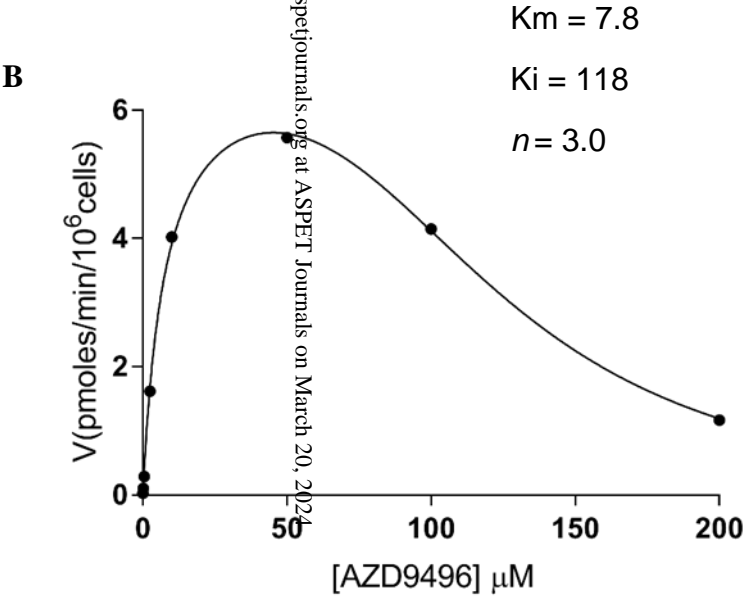
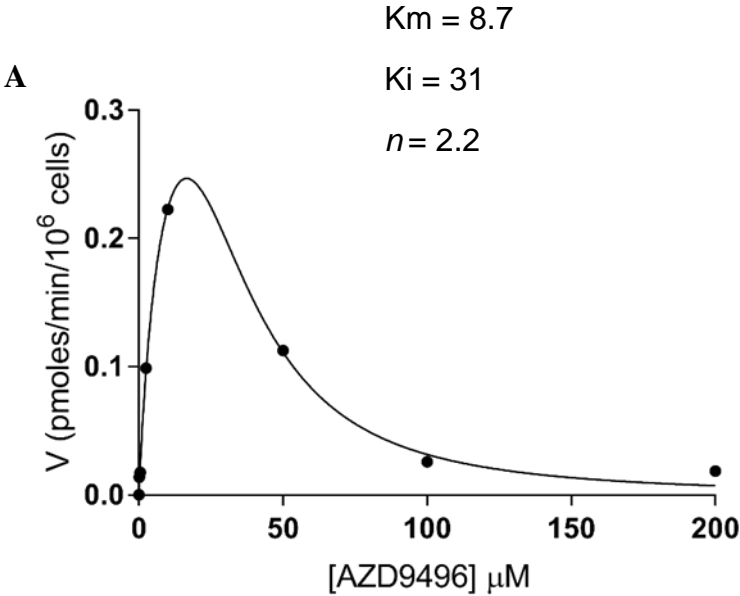


Figure 8

